行政院國家科學委員會專題研究計畫 期中進度報告

具新穎磁性之氧化物與特殊結構奈米金屬合成與特性分析(2/3)

期中進度報告(精簡版)

計 畫 類 別 ：個別型
計 畫 編 號 ：NSC 95-2113-M-002-009-
執 行 期 間 ：95 年 08 月 01 日至 96 年 07 月 31 日
執 行 單 位 ：國立臺灣大學化學系暨研究所

計 畫 主 持 人：劉如熹

報 告 附 件 ：出席國際會議研究心得報告及發表論文

處 理 方 式 ：本計畫可公開查詢

中 華 民 國 96 年 07 月 06 日

行政院國家科學委員會補助專題研究計畫成果報告

具新穎磁性之氧化物與特殊結構奈米金屬合成與特性分析(2/3)

計畫類別：■ 個別型計畫　□ 整合型計畫

計畫編號：NSC 95-2113-M-002-009

執行期間：95 年 8 月 1 日至 96 年 7 月 31 日

計畫主持人：劉如熹

共同主持人：

計畫參與人員：陳浩銘、郭慧通、沈錦昌、 黃景弘、
林群哲、郭恆嘉、劉耀閔

成果報告類型(依經費核定清單規定繳交)：■精簡報告　□完整報告

本成果報告包括以下應繳交之附件：

□赴國外出差或研習心得報告一份

□赴大陸地區出差或研習心得報告一份

■出席國際學術會議心得報告及發表之論文各一份

□國際合作研究計畫國外研究報告書一份

處理方式：除產學合作研究計畫、提升產業技術及人才培育研究計畫、列管計畫及下列情形者外，得立即公開查詢

□涉及專利或其他智慧財產權，□一年□二年後可公開查詢

執行單位：台灣大學化學系

中　華　民　國　96　年　5　月　15　日

行政院國家科學委員會專題研究計畫成果報告
具新穎磁性之氧化物與特殊結構奈米金屬
合成與特性分析(2/3)
Synthesis and Characterization of Novel Magnetic Oxides and Nano-Metal with Specific Structures

計畫編號：NSC 95-2113-M-002-009
執行期限：95 年 8 月 1 日至 96 年 7 月 31 日
主持人：劉如熹 教授（台灣大學化學系）

一、中文摘要

本研究以丹寧酸作為還原劑與包覆劑製備金/銀多角奈米結構，以紫外/可見光吸收光譜與延伸 X 光吸收細微結構研究其成長過程，其結果揭示以丹寧酸為還原劑將具非等向性成長之趨勢，金離子/銀原子之氧化還原反應與丹寧酸之還原將導致此一新穎金/銀奈米結構之生成。

關鍵詞：多角奈米結構、丹寧酸

一、Abstract

We describe here a novel method which shows that related large molecules, tannic acid, can control the morphology of silver/gold nanoparticles resulting in the formation of multipod-shaped nanostructures. In this work, multipod-shaped gold/silver nanostructures have been synthesized using tannic acid as reducing as well as capping agent. The growth process of gold/silver nanostructures have been studied by UV visible spectroscopy and extended X-ray absorption fine structure analysis. The reducing and capping properties of tannic acid favors the formation of unisotropic crystal growth. The growth of gold/silver nanostructures occurs as a consequence of the galvanic replacement reaction between Au^{3+}/Ag^{0} and subsequent reduction of both metal ions by tannic acid.

Keywords: Multipod-shaped nanostructures, Tannic acid

二、緣由與目的

There has been growing interest in biomimetic mineralization approaches for the creation of nanoscale materials with complex shape, controlled size shape and polymorph under ambient conditions in aqueous solutions.[1] These nanostructures exhibit very interesting electrical, optical, and chemical properties, which cannot be achieved by the corresponding bulk materials.Generally, spherical shaped inorganic nanoparticles (NPs) both semiconducting and metallic, have been of particular interest to the broad scientific community for decades. Fundamentally, in the case of semiconducting nanoparticles, the light that is absorbed and emitted can be tunable by diameter because the photogenerated electron-hole pair has an exciton diameter that is in the range of 1-10 nm scale.[2] For metallic nanoparticles, interesting optical and electronic effects are expected in the range of ~ 10-100 nm scales since the mean free path of an electron in a metal is 10-100 nm.[3] In addition, bimetallic nanoparticles have been considered to be valuable for investigating the relationship between the performance and their structures. Taton *et al.* reported that use of single-nanoparticles probes in recognizing DNA segments immobilized on a chip, when coupled with a signal amplification method based on promoted reduction of silver, the sensitivity exceeds that of the analogous fluorophore system by two orders of magnitude.[4]

三、研究方法

Sample Preparation. 50 mL of $AgNO_3$ aqueous solution (0.4 mM) was prepared, and then heated at 95 ℃ for 6 min. The reaction mixture was maintained at this temperature under magnetic stirring. Next, 5 mL of tannic acid (2%) was added into the $AgNO_3$ solution. After stirring for 10 min, silver nanoparticles were formed at this stage. Then desired volume of $HAuCl_4$ (25mM) solution as the source of Au^{3+} was injected into as-prepared solution of silver nanoparticles and kept stirring for 15 min. After reaction mixture was cooled to room temperature, the product was isolated by centrifugation and washed with water several times. For a hollow structure preparation, the colloidal nanoparticles were prepared by adding 5 mL of sodium citrate (1%) to 50 mL of silver metal salt ($AgNO_3$, 0.4 mM) solution. The solution was then heated at 95℃ in an oil bath for 15 min, and then 0.8 mL of 25 mM $HAuCl_4$ solution was added drop wise for another 15 min. The stirring was maintained throughout the synthesis. All experimental procedures were performed in open atmosphere.

Characterization. The UV/vis spectra of the colloidal nanoparticles solution were obtained using a SHIMADZU UV-1700 spectrophotometer with a

1cm quartz cell at room temperature. The surface morphology of the samples was studied by transmission electron microscopy (TEM). The specimens were obtained by placing many drops of the colloidal solution onto a Formvar-covered copper grid and evaporating it in air at room temperature. Prior to specimen preparation, the colloidal solution was sonicated for 1 min to improve the dispersion of particles on the copper grid. The samples used in the EXAFS measurement were prepared by concentrating 2000 mL of the previously obtained colloidal dispersions to 5~10 mL under nitrogen at reduced pressure. A series of EXAFS measurements of the synthesized samples were made using synchrotron radiation at room temperature. Measurements were made at the Au L_{III} edge (11918 eV) and the Ag K edge (25514 eV) with the sample held at room temperature.

四、結果與討論

TEM was used to image the Au/Ag polypod-like nanostructures. TEM micrographs of the Au/Ag nanopolypods after addition of 1.6 mL and 0.8 mL of $HAuCl_4$ solution to as-prepared silver nanoparticles is shown in Figure 1. The selected area electron diffraction pattern, shown as the inset in figure 1(b), indicates that the nano multipods have a face-centered cubic structure. As a matter of fact, the Au/Ag pods significantly increased as more volume of $HAuCl_4$ solution was added. Figure 1(c) shows 0.8 mL of $HAuCl_4$ solution was added to as-prepared silver nanoparticles solution in the presence of sodium citrate. As 0.8 mL of $HAuCl_4$ solution reacted with silver nanoparticles, the galvanic replacement reaction between Ag^0 and Au^{3+} occurred at this stage. This suggests that tannic acid acts as a growth inducing agent to form the multipod-shaped Au/Ag nanostructures, the Au/Ag nanopolypods cannot be observed in controlled experiments carried out without tannic acid.

Figure 2 shows the absorption spectra for the mixture of Au and Ag nanospheres, and after adding 1.6 mL and 0.8 mL of $HAuCl_4$ solution to as-prepared silver nanoparticles solution in the presence of tannic acid. The surface plasmon absorption spectra of gold nanorods are usually characterized by two bands. The absorption band appearing at the shorter wavelength is attributed to the transverse band, and that appearing at longer wavelength corresponds to the longitudinal band.[5] Spectrum of mixture of gold and silver nanoparticles also was shown in Figure2 (a) to confirm the formation of novel nanostructures. It should be noted that the positions of transverse and longitudinal bands were considerably different from that of usual gold nanorods and/or $Au_{core}Ag_{shell}$ nanorods, although the absorption spectra were similarly divided into two parts.[6] Generally, the thickly coated $Au_{core}Ag_{shell}$ nanorods show the longitudinal surface plasmon absorption at a much shorter wavelength than the thinly coated nanorods and the transverse plasmon absorption at similar wavelengths for both types of core-shell nanorods. In the present study, the longitudinal plasmon absorption of multipods nanoparticles prepared by using 0.8 mL of $HAuCl_4$ solution significantly shifted to the blue region suggesting more amount of silver deposition on the gold surfaces. The aspect ratio of nanopods prepared by using 1.6 mL of $HAuCl_4$ solution was larger than that of nanopods prepared by using 0.8 mL of $HAuCl_4$ solution, which results in the red shift of longitudinal plasmon absorption. As shown in figure 2a, after silver nanoparticles reacted with 1.6 mL $HAuCl_4$ solution, the longitudinal absorption band of 3D nanoploypods distributed over wider range as a result of an increase in the dimensions of the nanopolypods.

Figure 2 (b) shows absorption spectra of as prepared Ag nanoparticles and after addition of 0.8 mL of $HAuCl_4$ solution to these silver nanoparticles in the presence of sodium citrate. It was observed that the intensity of 398 nm Ag plasmon peak slightly reduced after addition of 0.8 mL of 25 mM $HAuCl_4$ solution. The reduction in the intensity can be attributed to the partial oxidation of silver nanoparticles even though only a simple electroless plating process was employed.

Figure 3 displays Au L_3 edge EXAFS oscillations of Au foil and multipod Au/Ag nanoparticles (after addition of 0.8 mL of $HAuCl_4$). An interesting change in oscillatory feature above ~ k = 5.5 $Å^{-1}$ was observed for Au coated with the silver shell. The arrow in the figure indicates oscillation caused by the presence of Ag for multipod nanoparticles suggesting that the spectral oscillation changed markedly with the deposition of silver atoms. This large difference facilitates the coordination analysis of the Au-Ag system. Figure 4 (a) presents the magnitude of the Fourier transform of Au L_3 edge $k^3\chi(k)$, where k = 3.0 ~ 14 $Å^{-1}$ of multipods Au/Ag nanoparticles. Evidently, a phase shift in $\chi(k)$ is seen, and Au-Ag in the first shell appears as a doublet in the Fourier transform of$\chi(k)$. The peak intensity at a lower distance exceeds than that at a higher distance because of the interference between silver and gold oscillations varies as Ag is deposited. It suggests that a significant amount of Ag is present in the nearest-neighbor shell around Au atoms. Thus, EXAFS analysis of multipod nanoparticles is characteristic of a two-component structure. Moreover, X-ray absorption spectrum of the Ag K edge was performed to provide further evidence of the presence of Ag atoms in multipod nanostructures (Figure 4b). As shown in Figure 4b, the FT-EXAFS spectrum of the Ag K edge of the multipod nanoparticles exhibits a distinct interference at the bimetallic interface in comparison with that of the Ag foil.

We must emphasize the fact that both presence of silver and tannic acid play important roles in the formation of multipod-shaped Au/Ag nanostructures. When the Au^{3+} ions were introduced into Ag nanoparticles solution, two critical reactions have to

be considered simultaneously. First, the galvanic replacement reaction between Au^{3+}/Ag^0 and second the reduction of both metal ions by tannic acid involved in growth of Au/Ag nanopods. In a typical displacement reaction, after adding Au^{3+} ions into Ag nanoparticles solution, Ag^0 atoms oxidizes to Ag^+ by Au^{3+} ions. After galvanic replacement reaction occurred, the Au^0 atoms and Ag^+ are formed. Moreover, the role of tannic acid as a reducing agent is very significant for the galvanic displacement which results in formation of both Au^0 and Ag^0 atoms.

Figure 5 summarizes all major steps involved in the galvanic replacement process and simultaneous reduction of metal ions by tannic acid and sodium citrate. In the case of tannic acid (path a), after $HAuCl_4$ solution has been added to the dispersion of silver nanospheres, tannic acid will start reducing gold ions in the solution. It results in the generation of seed sites on the surfaces of silver nanospheres to provide active sites for the subsequent growth. The first step would be the galvanic replacement process occurring at the interface of Ag^0/Au^{3+}. The released electrons in this process, can easily migrate to the surface of the nanoparticle and reduces $AuCl_4^-$ into Au atoms. The epitaxial deposition will lead to the formation of a crystal site on the surface owing to a good matching of crystalline structures and lattice constants between gold and silver. During this deposition, Ag^+ ions continuously diffuse out and dissolve in solution which result in the formation of gold-rich core due to dissolution of the silver core. In the second step, the dissolved silver ions are re-reduced to silver atoms by tannic acid which will then migrate to the nanopods surface. As a result of which, Au/Ag alloy is formed on the surface of nanopods. The generated gold and silver atoms continue to grow on the surface of nanopods and gradually emanate to form the multipod-shaped gold/silver nanostructure. As a matter of fact, Ag^+ ions will not precipitate as AgCl with Cl^- ions because the product of $[Ag^+]$ and $[Cl^-]$ was smaller than the solubility product of AgCl.[7] The silver chloride formed in this manner will be completely soluble in water under present experimental condition. In the presence of sodium citrate (path b), when the $HAuCl_4$ solution has been introduced into the dispersion of silver nanoparticles, the replacement reaction will start from the sites having relatively high surface energy. As a result, a hollow structure with a shell made of Au/Ag alloy is formed in this stage. The extension of this method would be viable to the other kinds of metal materials and is currently under study.

五、結論

Tannic acid-based one-pot synthesis of multipod-shaped gold/silver nanostructures has been described. We have shown that the amount of gold ions as well as the galvanic replacement between silver and chloroauric acid play important roles in the morphology control of the multipod-shaped nanostructures. It was found that the tannic acid acts as a reducing as well as capping agent in the synthesis of multipod-shaped nanostructures. Moreover, tannic acid favors the formation of unisotropic crystal growth. This methodology is expected to bring about new opportunities for the synthesis of new unisotropic metal nanostructures. This new nanostructure of the metal is expected to find use in a range of applications, especially in biology.

六、計畫成果自評

We have reached the goals of the research plan, some parts of the results have already publicized in scientific journals [8-28].

七、參考文獻

[1] P. Raveendran, J. Fu, and S. L. Wallen, "Completely Green Synthesis and Stabilization of Metal Nanoparticles", *J. Am. Chem. Soc.*, vol. 125, pp. 13940-13941, 2003.

[2] X. Peng, L. Manna, W. Yang, J. Wickham, E. Scher, A. Kadavanich, and A. P. Alivisatos, "Shape control of CdSe nanocrystals", *Nature* vol. 404, pp. 59-61, 2000.

[3] M. A. El-Sayed, "Some Interesting Properties of Metals Confined in Time and Nanometer Space of Different Shapes", *Acc. Chem. Res.* vol. 34, pp. 257-264, 2001.

[4] T. A. Taton, C. A. Mirkin, and R. L. Letsinger, "Scanometric DNA Array Detection with Nanoparticle Probes", *Science* vol. 289, pp. 1757-1760, 2000.

[5] K. L. Kelly, E. Coronado, L. L. Zhao, and G. C. Schatz, "The Optical Properties of Metal Nanoparticles: The Influence of Size, Shape, and Dielectric Environment", *J. Phys. Chem B* vol. 107, pp. 668-677, 2003.

[6] M. Liu and P. Guyot-Sionnest, "Synthesis and Optical Characterization of Au/Ag Core/Shell Nanorods", *J. Phys. Chem. B* vol. 108, pp. 5882-5888, 2004.

[7] Y. Sun, B. T. Mayers, and Y. Xia, "Template-Engaged Replacement Reaction: A One-Step Approach to the Large-Scale Synthesis of Metal Nanostructures with Hollow Interiors", *Nano. Lett.* vol. 2, pp. 481-485, 2002.

[8] H. M. Chen, H.-C. Peng, R. S. Liu, S. F. Hu, L.-Y. Jang, "Local Structural Characterization of

Au/Pt Bimetallic Nanoparticles", *Chem. Phys. Lett.* Vol. 420, pp. 484-488, 2006.

[9] H. M. Chen, R. S. Liu, L.-Y. Jang, J.-F. Lee and S. F. Hu, "Characterization of Core-shell Type and Alloy Ag/Au Bimetallic Clusters by Using Extended X-ray Absorption Fine Structure Spectroscopy", *Chem. Phys. Lett.*, 421, 118-123, 2006

[10] R. S. Liu, S. C. Chang, S. F. Hu and C. Y. Haung, "Highly Ordered Magnetic Multilayer Ni/Cu Nanowires", *Phys. Stat. Sol. (c)* 3, 1339-1342, 2006.

[11] H. M. Chen, H. C. Peng, R. S. Liu, S. F. Hu and H.-S. Sheu, "Morphology and Surface Plasma Changes of Au-Pt Bimetallic Nanoparticles, *J. Nanoscience and Nanotechnology* 6, 1411-1415, 2006.

[12] F. T. Huang, R. S. Liu and S. F. Hu, 2006, "Transformation of Co-nanodiscs to Caterpillars", *J. Mag. Mag. Mat.* 304, e19-e21, 2006.

[13] H. T. Chan, Y. Y. Do, P. L. Huang, P. L. Chien, T. S. Chan, R. S. Liu, C. Y. Huang, S. Y. Yang and H. E. Horng, "Preparation and Properties of Bio-compatible Magnetic Fe_3O_4 Nanoparticles", *J. Mag. Mag. Mat.* 304, e415-e417, 2006.

[14] F.-T. Huang, R. S. Liu, S. F. Hu, C.-L. Lee and A. K. Li, "Formation of Nano-structured Cobalt Wires with Chinese Caterpillar Type Structure", *J. Vac. Sci. Technol. B*, 24, 1440-1443, 2006.

[15] H. M. Chen, H. C. Lai, R. S. Liu and L.-Y. Jang, "Local Structural Characterization of Gold Nanowires Using Extended X-ray Absorption Fine Structure Spectroscopy", *Chem. Phys. Lett.* 428, 93-97, 2006.

[16] R. S. Liu, S. C. Chang, I. Baginskiy, S. F. Hu and C. Y. Huang, 2006, "Synthesis and Magnetic Properties of Multilayer Ni/Cu and NiFe/Cu Nanowires", *Pramana-Journal of Physics* 67, 85-91, 2006.

[17] H. M. Chen, R. S. Liu, K. Asakura, J.-F. Lee, L.-Y. Jang and S. F. Hu, "Fabrication of Nanorattles with Passive Shell", *J. Phys. Chem. B.* 110, 19162-19167, 2006.

[18] C. H. Kang and R. S. Liu, "The Effect of Terbium Concentration on the Luminescence Properties of Yttrium Oxysulfide Phosphor for FED Application", *J. Luminescence*, 122-123, 574-576, 2007.

[19] R. S. Liu and Y. S. Lin, "Chemical Substitution Effects of Tb^{3+} in YAG:Ce,Gd Phosphors and Enhancement of Their Emission Intensity Using Combination Flux", *J. Luminescence* 122-123, 580-582, 2007.

[20] Y. S. Lin Y. H. Tseng, R. S. Liu and J. C. C. Chan, "Luminescent Properties and the Host Structure of $Y_3Al_5O_{12}$:Ce Phosphors with Si_3N_4 Addititon", *J. Electrochem. Soc.* 154**,** 16-19, 2007.

[21] T. S. Chan, R. S. Liu, C. C. Yang, W.-H. Li, Y. H. Lien, C. Y. Huang and J. W. Lynn, "Neutron Diffraction Study of Multiferroic $Tb_{0.85}Na_{0.15}MnO_{3-y}$", *J. Mag. Mag. Mat.*, 310, 1151-1153, 2007.

[22] T. S. Chan, R. S. Liu, C. C. Yang, W.-H. Li, Y. H. Lien, C. Y. Huang, J.-F. Lee, "Chemical Size Effect on the Magnetic and Electrical Properties in the $(Tb_{1-x}Eu_x)MnO_3$ ($0 \le x \le 1.0$) System", *J. Phys. Chem. B*. 111, 2262-2267, 2007.

[23] Y. S. Tang, S. F. Hu, C. C. Lin, N. C. Bagkar and R. S. Liu, "Thermally Stable Luminescence of $KSrPO_4:Eu^{2+}$ Phosphor for White Light UV light-emitting Diodes", *Appl. Phys. Lett*. 90, 151108-1~3, 2007.

[24] H. M. Chen, C. F. Hsin, R. S. Liu, S. F. Hu and C. Y. Huang, "Controlling Optical Properties of Aluminum Oxide Using Electrochemical Deposition", *J. Electro. Chem. Soc.* 154, K11-14, 2007

[25] T. S. Chan, C. C. Kang, R. S. Liu, L. Chen, X.-N. Liu, J.-J. Ding, J. Bao and C. Gao, "Combinatorial Study of the Optimization of Y_2O_3: Bi, Eu Red Phosphors", *J. Com. Chem.* 9, 343-346, 2007.

[26] T. S. Chan, R. S. Liu, C. C. Yang, W.-H. Li,Y. H. Lien, C.Y. Huang, Jeff. W. Lynn, J. M. Chen, H. S. Sheu, "Influence of Oxygen Defects on the Crystal Structure and Magnetic Properties of the $(Tb_{1-x}Na_x)MnO_{3-y}$ ($0 \le x \le 0.3$) System, *Inorg. Chem.* 46, 4575-4582, 2007.

[27] R. S. Liu, H. M. Chen and S. F. Hu, "Synthesis and Characterization of Long Gold Nanorods, IEEJ Trans. 2, 1-5, 2007.

[28] H. M. Chen, C. F. Hsin, R. S. Liu, J.-F. Lee, and L.-Y. Jang, "Synthesis and Characterization of Multi-Pod-Shaped Gold/Silver Nanostructures", *J. Phys. Chem. C* vol. 111, pp. 5909-5914, 2007.

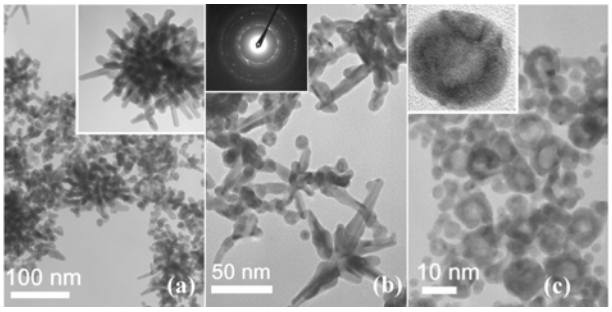

Fig. 1. TEM micrographs of the Au/Ag nanopolypods under different volume of $HAuCl_4$ solution reaction condition. (a) 1.6 mL and (b) 0.8 mL of $HAuCl_4$ solution were added to as-prepared silver nanoparticles solution under presence of tannic acid. (c) 0.8 mL of $HAuCl_4$ solution was added to as-prepared silver nanoparticles solution under presence of sodium citrate.

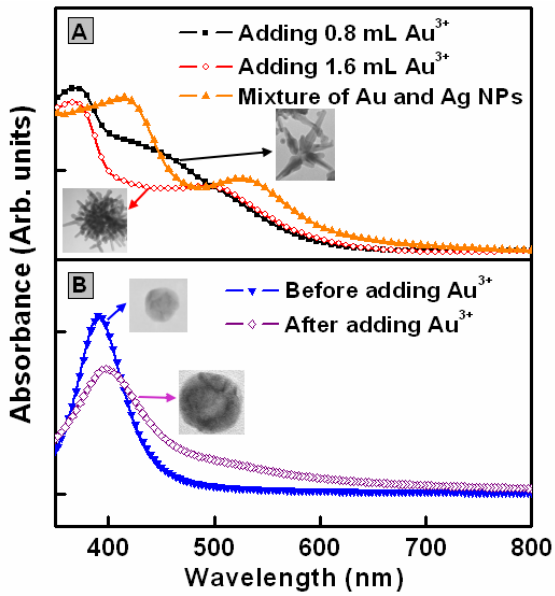

Fig. 2. (a) Extinction spectra of mixture of Au and Ag nanospheres. Au/Ag nanopolypods after adding 0.8 mL and 1.6 mL of $HAuCl_4$ solution to as-prepared silver nanoparticles solution. (b) As-prepared Ag nanoparticles and 0.8 mL of $HAuCl_4$ solution was added to these silver nanoparticles solution in the presence of sodium citrate.

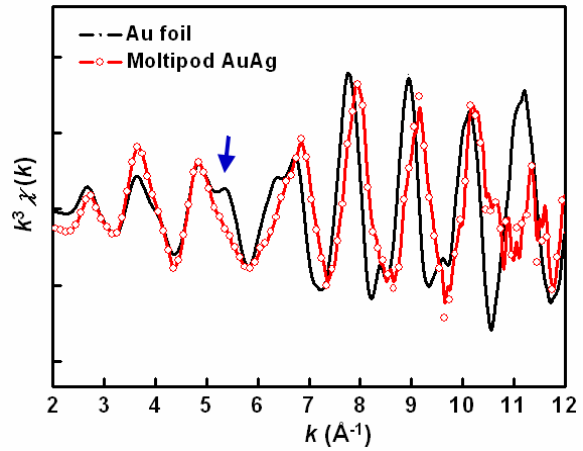

Figure 3. Au L_3 edge EXAFS oscillations for Au foil and multipods Au/Ag nanoparticles (0.8 mL of $HAuCl_4$ was added). The arrow indicates oscillation caused by the presence of Ag.

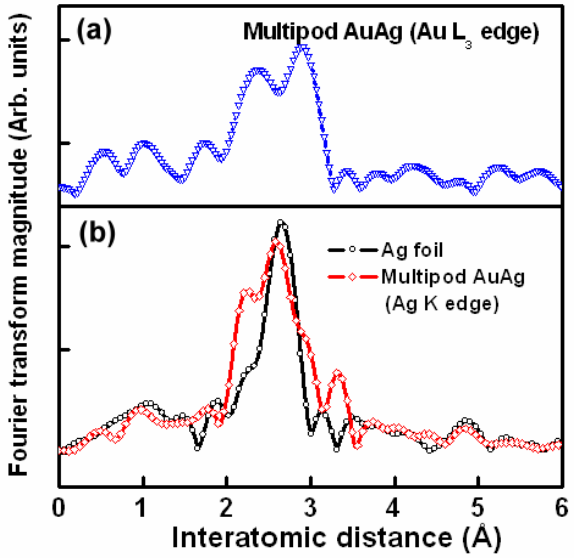

Figure 4. (a) Fourier transforms of Au L_3 edge $k^3\chi(k)$ EXAFS spectrum of multipods Au/Ag nanoparticles. (b) Fourier transforms of Ag K-edge $k^3\chi(k)$ spectrum of Ag foil and multipods Au/Ag nanoparticles.

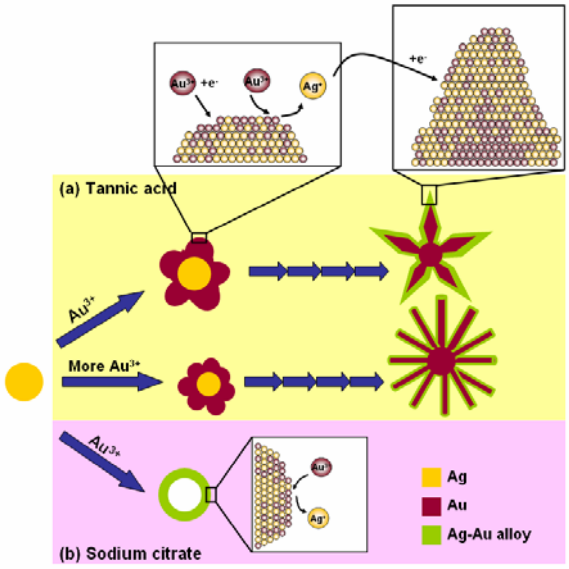

Figure 5. Schematic illustration summarizing all reaction and structural changes involved in the galvanic replacement reaction. (a) Prepared under presence of tannic acid. (b) Prepared under presence of sodium citrate.

出國報告

報告人：劉如熹 (台灣大學化學系)

會議經過:

2007年氫能及燃料電池國際會議(Hydrogen & Fuel Cells 2007)於四月二十九日至五月二日於加拿大溫哥華之Vancour Convention & Exhibition Center召開。會議主席由Dr. John Tak (President and CEO, Hydrogen & Fuel Cells Canada)籌畫與召開，並由另外三位會議主席協助，其分別為Christopher Curtis (Vice President, Hydrogen & Fuel Cells Canada)、Nick Beck (S&T Director, Hydrogen, Fuels and Transportation Energy, Natural Resources Canada)與Greg Reimer (Deputy Minister, BC Ministry of Energy, Mines Resources and Petroleum Resources)。會議主要分為氫能與燃料電池兩大主題，於四天之議程中含Keynote Address、oral presentation 與 poster。計約700餘人與會，其屬相當大型之會議。

重要討論結果如下所示：

Dr. Anthony Freeman (Program Manager, Earth Science Research and Advanced Concepts, NASA, USA)首先指出導致氣候變遷，乃源自化石燃料的二氧化碳，在近幾年正以超乎預期的高速度攀升。平均二氧化碳的年成長率，在1990年代是1.1%，而在2000年代則升高為3%。在2005年，有接近80億公噸的二氧化碳被排放到大氣裡，比較而言，於1995年約是60億公噸。最主要促成二氧化碳排放量急遽增加的原因，乃因於全球為增加每一元所得所產生的二氧化碳提高。在過去幾年，化石燃料的使用確實減少，現在的壓力是來自持續成長的人口與人民所得。在一個國家走向工業發展時，它也正密集但無效率使用化石燃料。能源使用效率藉由經濟發展而改善，但最後也只是彌補之前的無效率。工業化國家－例如加拿大、澳洲與美國－即處在此彌補時期。但開發中國家－例如中國大陸－則處在密集發展的階段。考慮以上因素，事實上全球的化石燃料使用上的效率依然是在降低的。中國的每人二氧化碳排放量依然是低於全球平均值。平均而言，澳洲與美國目前每年每人排放約5公噸的二氧化碳，而中國則為1公噸。在工業革命之後的兩個世紀，美國與歐洲總共排放超過50%的全球二氧化碳，而中國則低於8%，另外約50個已開發國家的貢獻小於0.5%。根據跨政府氣候變遷組織[Intergovernmental Panel on Climate Change (IPCC)] 所採用的化石燃料使用準則，最近幾年的二氧化碳排放量已經走到高峰的盡頭。二氧化碳排放量是有歷史性的。一般必須考量過去與現在排放量的趨勢，才能談全球二氧化碳是否有下降的趨勢。

綜合Mr. Bill Reinert (National Manager, TMS advanced Technologies Group, Toyota Motor Company)談Toyota's Fuel Cell Program、Dr. Christine Sloane (Glogal Leader & Director of Hydrogen Fuel Cell Codes and Standards, General Motors Corp)給GM Fuel Cell Vehicles: Moving Forward之演講、 Mr. Chris Guzy (Vice President & Chief Technology Officer, Ballard Power Systems)提供Making Fuel Cells a Commerical Reality之演講、Mr. Alison Setton (Manager, Vancourver Fuel Cell Vehicle Program)講The Vancourver Fuel Cell Vehicle Oroject等其結論如下：

由於化石能源短缺、溫室效應日益嚴重，世界各國均致力於減少溫室效應氣體並開發新興能源。新能源是只傳統石油燃料以外的能源，包括氫能及再生能源，具有潔淨、低汙染且可循環再生的特點，而未來氫能的開發與應用將是最重要的項目之一。1997年聯合國世界氣候會議發表京都議定書，經各國首長陸續簽

署後，於2005年正式生效，世界二氧化碳及其他如甲烷、氮化物、鹵化物等溫室氣體的排放量須逐年削減，京都議定書生效後更刺激新能源產業的發展。所謂新能源是指氫能與再生能源，其特性為可再生循環並大幅降低二氧化碳排放量與其他汙染。氫能源技術開發與應用，將是重要的發展項目之一，因為氫反應的主要產物是水，具有低污染的優點，且氫能屬於二次能源，在大自然中含量豐富且再生周期短，可不斷循環利用，只要能克服生產、儲存、輸送與應用等技術上的困難，便能發展出效率更高且多元化的永續能源供需系統。

使用氫燃料的內燃機（Hydrogen-Fueled Internal Combustion Engines,H_2ICEs），簡稱氫引擎(Hydrogen Engines)。直到近代各大車場再度重視氫引擎，例如福特、通用汽車、Mercedes-Benz，BMW等著名車場，均推出以氫能做為燃料的汽車，但只限於原型車及少量試用階段。例如美國首都便有一處由Shell石油公司與通用汽車合作設立的加氫站，由通用汽車免費提供6台以氫引擎為動力的汽車供人使用。加拿大成立Hydrogen Early Adopters計畫，耗資850萬美元，已有10輛巴士於加拿大正式上路運作。此計畫並非以獲利為目的，而是為地球的未來催生更乾淨的車輛。

綜合Mr. Christopher Curtis (Vice President, H2FCC)談The German National Development Plan for the Hydrogen and Fuel Cell Technology Innovation Programme)、Mr. Line Hagen (Director Research, The Research Council of Norway)給The First Norwegian Action Plan on – Strengthening the Effort on Hydrogen and Fuel Cells in Norway之演講、 Mr. Aksel Mortensgaard (Head of Section, Energy R & D, Danish Energy Authority)提供Fuel Cells in Danmark之演講、Dr. Tetsuya Kogaki National Institute of Advanced Industrial Science and Tecnhnology (AISt), Japan)講Japan's Strategies, Policies and Programs Related to the Commercialization of Hydrogen and Fuel Cell Technology等其結論如下：

氫能是高能量密度且潔淨的燃料，若僅用於燃燒，其能源轉換效率會因為大部分的能量轉換成熱損失而降低。但若使用燃料電池，以氫氣為燃料、空氣為氧化劑，經氧化還原反應後將能量轉換為直流電，則可提高能源轉為電力的效率。傳統發電系統的平均熱效率低於40％，若改以天然氣及空氣為燃料，產氫供應燃料電池，其發電效率可超過40％，固態氧化物燃料電池的發電效率甚至可達60％以上，對於減少CO_2排放將有很大的貢獻。

1960年代科學家即看好燃料電池的高效率特性在未來的發展潛力，但由於當時的石化燃料不虞匱乏、價格低廉，加上燃料電池發電技術成本遠比傳統大型發電技術高，因此燃料電池多應用於太空梭、潛水艇等用途。燃料電池技術發展至今，依使用之電解質分為：鹼性燃料電池(Alkaline Fuel Cell,AFC)、磷酸燃料電池(Phosphoric Acid Fuel Cell,PAFC)、熔融碳酸鹽燃料電池(Molten Carbonate Fuel Cell,MCFC)、固態氧化物燃料電池(Solid Oxide Fuel Cell,SOFC)、直接甲醇燃料電池(Direct Methanol Fuel Cell,DMFC)、質子交換膜燃料電池(Proton Exchange Membrane Fuel Cell,PMEFC)等。為因應氫引擎與燃料電池的需求，必須有氫氣供應系統的配合。依供應鏈不同，產氫系統可分為集中式產氫(centralization)與線上產氫(on-board,on-site)兩種方式。前者偏向大量產生純氫，經由容器儲存後，可快速補充氫引擎或燃料電池車輛所需的氫燃料，由於所產出的氫能並非立即使用，因此又稱為離線式(off-site)產氫；後者則偏向線上直接生產、流量需求較低，氫能可被立即使用的富氫氣體生產技術。

水電解產氫法乃直接以外加電場的方式電解水，將處於穩定態的水分解為氫

氣與氧氣。事實上，以水電解產生氫較不經濟，但可利用離峰時段多餘的電力，或由太陽能、風力等不穩定的自然能發電用於電解產氫，將之儲存為氫能，用於燃料電池即為穩定的電力來源。

目前氫能還無法大量使用的原因，在於其運送及儲存的技術瓶頸，氫氣儲存需考量許多因素，例如安全性、價格、重量、能量密度等。目前的儲氫方法大致上有四種：高壓儲氫、液態儲氫、儲氫合金及吸附儲氫。一般運輸大量氫燃料以高壓儲氫及液態儲氫居多，但在燃料電池應用方面的發展趨勢，則是以高壓儲氫與儲氫合金為主。線上產氫技術目前則以重組器搭配PEMFC為主流，不論是定置型或攜帶型。儲氫技術目前則以高壓儲氫為主，液態儲氫則有逐漸與高壓儲氫並行得趨勢，這兩種儲氫技術仍以大量使用與儲存為主。燃料電池實用化已非遙不可及的夢想，經各國研發菁英的努力，燃料電池實際應用於電動汽車及分散式定置型家用發電系統，已達到初期推廣測試的階段，而成本、使用壽命、系統穩定性、啟動速度、能量密度輸出等問題，也因各方投注心力而於近年內獲得改善。

參加心得：

由此會議可知其他可採行的替代石化能源，，而替代能源必須是能源源不絕地供應人類的需求，如水力發電、核電、風力渦輪，甚至發展生質柴油等，可用於供應汽車的能源。目前已知由水及石化燃料中，找出許多氫利用做為替代能源的可能性，氫元素是製造水的一種很乾淨的物質，且可以用為製造能源的副產品。

加拿大一直以來是全球氫科技及燃料的領導國家，溫哥華市則有世界最大的燃料組織研究群，有超過2000名的研究人員在此從事燃料能源的研究。然而，到底氫元素能源何時可以普及呢？這就要看如何去應用，很多新的研究不斷地進行中，每年都會有不同的研究結果發表，若以眼睛看得見的東西而言，像是自動化的商品使用就是一個極大的商業市場，然而成本必須要低，可靠性和耐久性也必須要高才行。

氫元素能源也可做為備電池的使用，像是電話手機的基地台以及資料庫中心等，研究成果的最終目的是要推廣於商業化的應用，譬如手機用的氫電池，可以延長手機10～20小時的使用，而此項成本是目前使用的能源，如煤炭或天然氣廠的二到五倍，故仍必須將成本降低。加拿大國家研究院正在進行氫燃料開發研究使用。氫氣能源是一種因接觸反應作用而使電子釋出，也就是一種電力，一種質子交換的薄膜(Proton Exchange Membrane: PEM)燃料。在自動化的應用上，PEM是一種十分理想的元素，因為它很輕且密度緊密結實。

會議中本人亦發表題為: Reaction Mechanism of Pt-$LiCoO_2$ Catalysed Hydrolysis of Sodium Borohydride for Fuel Cell論文，本研究主要乃藉由數種分析技術探討化學氫反應之特性與觸媒催化反應機制。其中所涵蓋之方法包括：以X光粉末繞射法 (X-ray diffraction；XRD) 鑑定樣品之純度與分析其晶體結構；以穿透式電子顯微鏡(transmission electron microscopy；TEM) 進行樣品表面型態、粒徑大小與分布、表面成分以及原子排列之晶格影像分析；以X光吸收光譜(X-ray absorption spectroscopy；XAS) 之X光吸收邊緣結構 (X-ray absorption near edge structure；XANES) 決定樣品中元素之價數與電子結構以及延伸X光吸收精細結構 (extended X-ray absorption fine structure；EXAFS) 瞭解吸收原子周圍之原子級短程有序結構；以感應耦合電漿-原子發射光譜儀 (inductively coupled plasma-atomic emission spectrometer；ICP-AES)鑑定含浸於載體上之白金量；以振動樣品磁力計(vibrating sample magnetometer；VSM)量測觸媒於產氫反應前後之

磁特性。此結果得到各國代表專家之重視，此次並與各國專家充分交換研究心得，對未來之發展認識有極佳之助益，於此感謝國科會之補助。

攜回資料:

大會議程及論文摘要一份。

Reaction Mechanism of Pt-$LiCoO_2$ Catalysed Hydrolysis of Sodium Borohydride for Fuel Cell

R. S. Liu, [*,1] H. J. Lei,[1] N. C. Bagkar,[1] J.-F. Lee,[2] H. J. Chuang,[3] S. M. Chaung[3] and B. J. Weng[3]

[1]Department of Chemistry, National Taiwan University, Taipei, 106 Taiwan, [2]National Synchrotron Radiation Research Center, Hsinchu, 300 Taiwan, [3]Chung-Shan Institute of Science and Technology, Taoyuan, 325 Taiwan.

Abstract

The synthesis of platinum nanoparticles loaded on $LiCoO_2$ was successfully carried out by impregnation method followed by sintering at different temperatures. The catalytic role of Pt-$LiCoO_2$ composite in hydrogen generation during hydrolysis of sodium borohydride ($NaBH_4$) was studied for fuel cell application. The hydrogen generation rates were determined to measure the catalytic activities for the hydrolysis of $NaBH_4$ using different concentrations of platinum nanoparticles loaded on $LiCoO_2$ support. It was found that the 15 wt.% of Pt nanoparticles on $LiCoO_2$ sintered at 450 ^oC support showed the maximum efficiency for catalysis reaction of hydrogen production. Synchrotron radiation source and X-ray absorption was used in order to understand the mechanism of catalytic process for the production of hydrogen during the hydrolysis of $NaBH_4$. Based on X-ray absorption near edge (XANES) results, we propose the mechanism for the hydrogen generation using Pt-$LiCoO_2$ catalyst which involves the discharge of the electron through the catalyst to the $LiCoO_2$ support resulting in simultaneous oxidation and reduction of hydrogen ions from BH_4^- and water respectively leading to generation of hydrogen.

Introduction

In recent years, fuel cell systems using liquid fuels, such as the direct methanol fuel cell (DMFC) and direct borohydride fuel cell (DBFC), are considered future technology for mobile and portable power supplies as replacement for existing batteries. The direct borohydride fuel cell (DBFC) system, with $NaBH_4$ solution as the fuel has attracted attention since the late 1990s for application in portable power supplies due to its higher specific energy and more compact structure than the DMFC system. Metal hydride salts such as $NaBH_4$ constitute safe and practical hydrogen reservoirs for PEM fuel cells [1-3]. The hydride is non-toxic, non-inflammable, produces pure hydrogen, and carries a superior weight and volumetric capacity for hydrogen delivery. It has high storage density upto 10.8 wt% for hydrogen, stability in air, easily controlled hydrogen generation rate and side product recyclability [4]. Hydrolysis of sodium borohydride, usually with a precious metal catalyst, is a promising method for hydrogen generation in fuel cell applications. Hydrogen can be generated in a double amount of its stored content by controllable heat releasing reaction with no side reaction or volatile byproducts and generated hydrogen is very high purity which can be combined with proton exchange membrane (PEM) fuel cell application.

The hydrolysis of $NaBH_4$ in aqueous solution in the presence of catalyst can release hydrogen rapidly in the following way:

$$NaBH_4 + 2H_2O \rightarrow NaBO_4 + 4H_2 + 217\ kJ \quad (1)$$

The limitations of the hydrolysis of sodium borohydride are sluggish reaction rate due to decrease in the pH of the solution on account of formation of sodium metaborate and the self hydrolysis of sodium borohydride at low pH value results in the uncontrolled release of hydrogen [5]. These difficulties are overcome by increasing the pH of the solution above 9. The role of heterogeneous catalyst is to produce hydrogen from alkaline solution of sodium borohydride since in the absence of catalyst it does not produce appreciable quantities of hydrogen. The catalyst generally used for the hydrolysis of sodium borohydride include colloidal metal clusters of noble metals, active carbon, metal halides, metal nanoparticles supported on ion exchange resin beads [6].

The objective of the present investigation is to synthesize an active Pt catalyst impregnated on metal oxide such as $LiCoO_2$ surfaces and to probe the structural and local environmental changes occurring in the vicinity of both active Pt catalyst as well as $LiCoO_2$ support during the heterogeneous catalysis of hydrolysis of sodium borohydride. We have used X-ray absorption utilizing X-ray absorption near edge structure (XANES) measurements for probing the structural and local environmental changes occurring in the vicinity of the active catalyst. The use of XANES using synchrotron radiation gives valuable information about the changes in the local structural environment of the absorbing atom.

2. Experimental

All chemicals, H_2PtCl_6 (99.5 %) from Alfa, $LiCoO_2$ (99.8 %) from Aldrich, sodium borohydride (99.0 %) from Aldrich, nafion (5 %) Dupont, Pt/C (5 %) from Acros were used without further purification. The platinum nanoparticles loaded $LiCoO_2$ composite catalyst samples were synthesized by mixing H_2PtCl_6 and $LiCoO_2$ in a desired ratio such that concentration of Pt varies as 5, 15 and 30 %. The composite samples were then heated after sonication for 20 mins in the furnace at 250 ^oC for 5 h in air atmosphere. The catalyst samples were then sintered in air atmosphere at 450 ^oC for 5 h. The catalytic process was monitored by measuring hydrogen generation rates for the hydrolysis of $NaBH_4$ using catalysts. In a typical experiment 0.1 g of sodium borohydride and 10 mg of Pt-$LiCoO_2$ were mixed in stoppered flask and to this 25 ml of deionized water was added. The hydrogen generated during the hydrolysis of $NaBH_4$ was collected and its volume was measured using water trap method at the time interval of 5 min.

2.1 Characterization

X-ray diffraction (XRD) measurements were carried out using BL17A1, synchrotron radiation X-ray source at National Synchrotron Radiation Research Centre. The surface morphology was examined by transmission emission microscope (TEM) using JEM-2000EX microscope operated at 200 kV. The Co *K*-edge X-ray absorption near-edge structure (XANES) was recorded in transmission mode for synthesized powder mounted on Scotch tape, at a BL17C Wiggler beamline by using a double-crystal Si (111) monochromator. Wiggler-C beamline of the National Synchrotron Radiation Research Center (NSRRC), Taiwan, has been used for such experiments.

3. Results and Discussion

TEM image and electron diffraction pattern of 15 wt% of Pt-$LiCoO_2$ is shown in Fig. 1. It shows the nanoparticles of Pt dispersed in $LiCoO_2$ support with a uniform particle size distribution with an average particle size of 3.7 ± 0.8 nm.

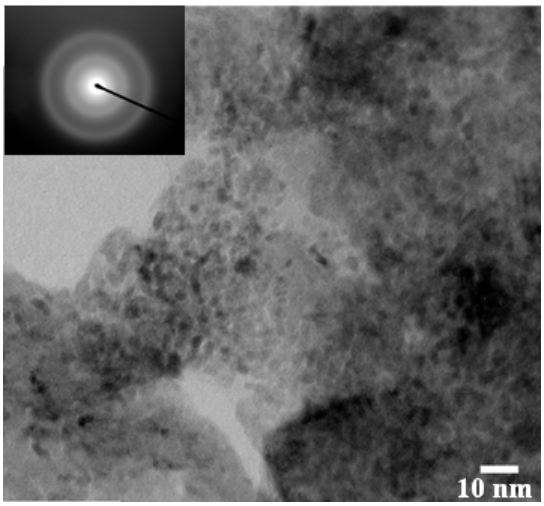

Fig. 1 TEM image and electron diffraction pattern of 15 wt% Pt-$LiCoO_2$

It was observed that the particle size and density distribution is increased for higher Pt concentration and 15 wt% Pt-$LiCoO_2$ composite catalyst showed more narrow size distribution amongst others in the support. Hydrogen generation experiments were carried out to find out the catalysis effect of Pt-$LiCoO_2$ composite. Fig. 2 shows the volume of hydrogen generated for 5, 15, 30 wt% of Pt-$LiCoO_2$. It was observed that 15 wt% Pt-$LiCoO_2$ showed the maximum hydrogen generation rate suggesting the optimum concentration of Pt for catalysis of sodium borohydride. The reduction in the surface area due to aggregation of platinum nanoparticles causes the decreased hydrogen generation rate for higher concentration.

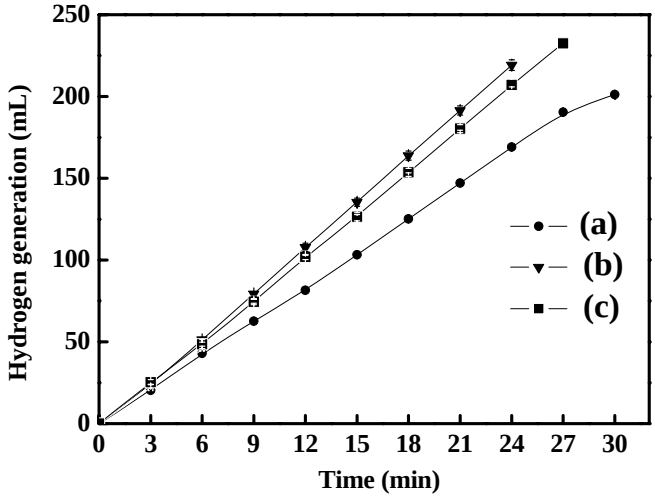

Fig. 2 Hydrogen generation of (a) 5, (b) 15, (c) 30 wt% of Pt-$LiCoO_2$.

The hydrogen generation using 5 wt% Pt-$LiCoO_2$ and $LiCoO_2$ follows zero order kinetic dependence with hydrogen generation rate of 2.0 x 10^{-5} g/s and 8.61 x 10^{-5} g/s for pure $LiCoO_2$ and 5 wt% Pt-$LiCoO_2$, respectively. It suggests us that the rate is independent of sodium borohydride concentration and depends on the surface area of the catalyst.

We have used 15 wt% Pt-$LiCoO_2$ for *ex situ* analysis of Pt-$LiCoO_2$ catalysed hydrolysis of sodium borohydride using synchrotron radiation source since it gives

the maximum H_2 generation rate. XRD measurements using synchrotron beamline BM01C2 were carried out on pure $LiCoO_2$ and 15 wt% Pt-$LiCoO_2$ to study the role of catalyst during hydrolysis. Fig. 3 shows the XRD pattern of 15 wt% Pt-$LiCoO_2$ compared with pure $LiCoO_2$, Co and Pt foil. The structure of pure $LiCoO_2$ during the hydrolysis for different time periods remains the same whereas the XRD pattern of Pt-$LiCoO_2$ showed remarkable changes with time. Pt plays an important role as an active centre during the hydrolysis causing the reduction of Co^{3+} ions to Co metal through the electron transfer as indicated by a peak in Fig. 3.

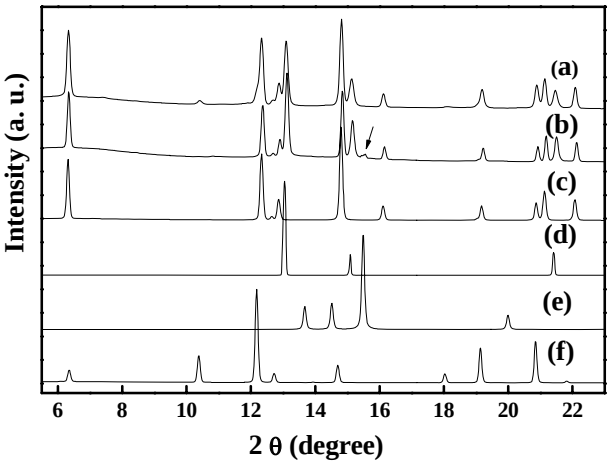

Fig. 3 XRD patterns of 15 wt% Pt-$LiCoO_2$ (a) before, (b) after catalysis reaction compared with pure (c) $LiCoO_2$, (d) Pt foil, (e) Co and (f) Co_3O_4.

The role of Pt can be understood as a mediator during the reaction causing efficient electron transfer during the hydrolysis. The concentration of BH_4 ions in the vicinity of catalyst surface decreases during the hydrogen generation and more BH_4 ions should absorb on the Pt surface which will be helpful for the electron transfer from BH_4 to $LiCoO_2$ liberating hydrogen. The catalysis of platinum during the hydrolysis was studied by X-ray absorption studies on pure $LiCoO_2$ and 15 wt% Pt on $LiCoO_2$ during the hydrolysis of sodium borohydride. Fig. 4 shows the *ex situ* Co *K*-edge XANES for pure $LiCoO_2$ and 15 wt% Pt-$LiCoO_2$ before and after at 1 and 5 h of reaction time completion. It was observed that there is no shift in the XANES pattern for pure $LiCoO_2$ for the reaction time of 1 hr completion. The XANES spectra of 15 wt% Pt on $LiCoO_2$ changed to lower energy values with time indicating the formation of Co metal as the reaction proceeds. The shift in the near edge region suggests that Pt nanoparticles played a major role causing the reduction of Co^{3+} to Co metal with liberation of hydrogen.

We propose the mechanism of overall catalysis process of hydrogen production using Pt-$LiCoO_2$ by using the results obtained from structural investigation. The active nanocentres of Pt are surrounded by BH_4 ions because of high molar ratio of [BH_4] / [Pt] which causes easy removal of H ions from BH_4 ions as a result of electron transfer form BH_4 ions through the catalyst in the first process. In this case, Pt or Co ions in the composite absorbed the electrons and results in the formation of metallic species by reduction of the metal ions as indicated by XANES measurements. The role of platinum is very crucial in the charge transfer process as there is no evidence of Co reduction using pure $LiCoO_2$ as a catalyst from XANES Co *K*-edge analysis.

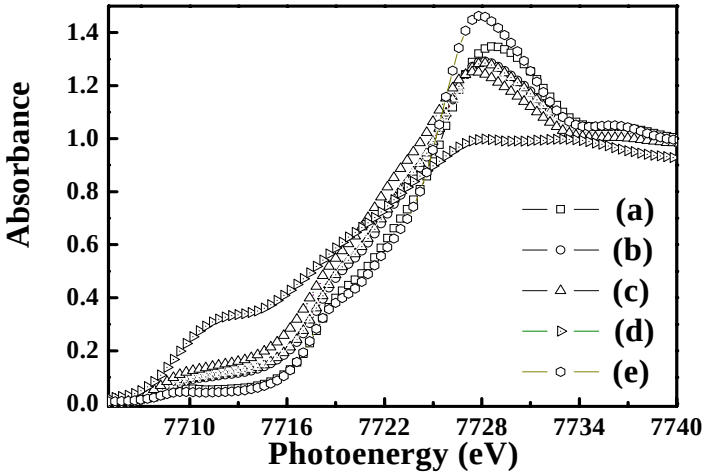

Fig. 4 The *ex situ* Co *K*-edge XANES of 15 % Pt-$LiCoO_2$ (a) before, (b) 1 h, (c) 5 h of reaction completion, (d) Co foil and (e) $LiCoO_2$.

Pt acts as a mediator in electron transfer causing the increased metal content which may be beneficial for the regeneration of the catalyst surface. Thus *ex situ* XANES investigations of the composite catalyst provided the valuable information about the structural changes occurring during the hydrolysis reaction.

4. Conclusions

The synthesis of Pt-$LiCoO_2$ composites was carried out successfully using impregnation method and the catalytic activities were investigated by hydrogen generation rates. The characterization using XRD and TEM confirmed the nanoparticles of Pt loaded on $LiCoO_2$. 15 wt% Pt-$LiCoO_2$ was found to be effective catalyst for the hydrogen production as suggested by higher generation rates. XRD and XANES using synchrotron radiation source *ex situ* studies showed the changes in the local structure of absorbing Pt and Co atom during the catalysis reaction. XANES results suggest electron transfer through the catalyst to the $LiCoO_2$ support resulting in generation of hydrogen.

Acknowledgements

The authors would like to thank the National Science Council of Taiwan (contract No. NSC 95-2113-M-002-009) and the Chung-Shan Institute of Science and Technology for financially supporting this research.

References

1. Y. Suzuki, *Int. J. Hydrogen Energy*, 1982, **7**, 227.
2. H. I. Schlesinger, H. C. Brown, A. E. Finholt, J. R. Gilbreath, H. R. Hoekstra and E. K. Hyde, *J. Am. Chem. Soc.*, 1953**, 75**, 215.
3. V. Kong, C. Y. Foulkes, F. R. Kirk and D. W. Hinatsu, *Int. J. Hydrogen Energy*, 1999, **24**, 665.
4. J.-H. Kim, H. Lee, S.-C. Han, H.-S. Kim, M.-S. Song and J.-Y. Lee, *Int. J. Hydrogen Energy*, 2004, **29,** 263.
5. S. C. Amendola, P. Onnerud, M. T. Kelley and M. Binder, *Talanta*, 1999, **49**, 267.
6. S. C. Amendola, S. L. Sharp-Goldman, M. S. Janjua, N. C. Spencer, M. T. Kelley, P. J. Petillo and M. Binder, *Int. J. Hydrogen Energy,* 2000, ***25***, 969.

Curriculum Vitae:

Professor Ru-Shi Liu received his Bachelor degree in Chemistry from Shoochow University (Taiwan) in 1981. He got his Master Degree in nuclear science from the National Tsing Hua University (Taiwan) in 1983. He obtained two PhD degrees in Chemistry from National Tsing Hua Univeristy in 1990 and from University of Cambridge in 1992. He joined Materials Research Laboratories at Industrial Technology Research Institute as a Associate Researcher, Research Scientist, Senior Research Scientist and Research Manager from 1983 to 1985. Then he became an Associate Professor at the Department of Chemistry of the National Taiwan University from 1995 to 1999. Then he promoted as a Professor in 1999. He got the Excellent Young Person Prize in 1989, Excellent Inventor Award (Argentine Medal) in 1995 and Excellent Young Chemist Award in 1998. Professor Liu's research interest lies in the Materials Chemistry. He is the author and coauthor of more than 300 publications in scientific international journals. He has also granted more than 60 patents.